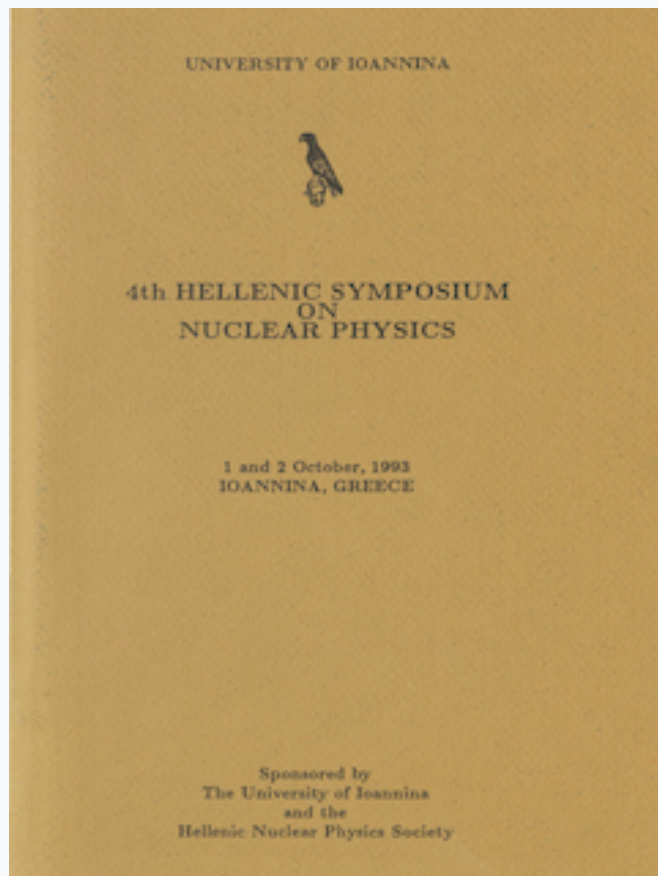


# HNPS Advances in Nuclear Physics

Vol 4 (1993)

HNPS1993



## Total Cross Section of the n+11B Reaction

G. Galios, G. Doukelis, S. Kossionides, T. Paradellis

doi: [10.12681/hnps.2870](https://doi.org/10.12681/hnps.2870)

### To cite this article:

Galios, G., Doukelis, G., Kossionides, S., & Paradellis, T. (2020). Total Cross Section of the n+11B Reaction. *HNPS Advances in Nuclear Physics*, 4, 13–20. <https://doi.org/10.12681/hnps.2870>

# TOTAL CROSS SECTION OF THE $n+^{11}B$ REACTION

*G.GALIOS, G. DOUKELLIS, S. KOSSIONIDES and T. PARADELLIS*

## Abstract

*The total neutron cross section of  $^{11}B$  has been measured from 7.2 to 8.4 MeV. The analysis of all data from the  $^8Li(\alpha, n_0)^{11}B$  reaction in combination with the total cross section data can determine an upper limit on the stellar reaction rate of the  $^8Li(\alpha, n)^{11}B$  reaction.*

## 1. Introduction

An important result, for the nucleosynthesis period in the early universe, from inhomogeneous big bang models is the production of heavier than  $^7Li$  elements. In these models the major pathway [1] for this process passes through the  $^8Li(\alpha, n)^{11}B$  reaction. This important reaction has been investigated in the astrophysically interesting energy region, first time [1] via the inverse reaction  $^{11}B(n, \alpha)^8Li$ . Measurements with better neutron resolution and smaller neutron energy step have been done in recent years [2]. Using the principle of detailed balance the data were converted to cross sections or S-factor of the  $^8Li(\alpha, n_0)^{11}B$  inverse reaction (only for neutron decay to the ground state in  $^{11}B$ ). The analysis of these data has shown [2] two broad components and three narrow ones. The parameters of these resonances are listed in table 1.

The 10525 keV and 10638 keV states of  $^{12}B$ , that have the main contribution to the reaction rate of ( $^8Li + \alpha$ ) have not been observed in other reactions [6,7], while Fossan et al [3] measurements and Auchampaugh et al [4] in more recent reference of total neutron cross section in  $^{11}B$  indicate the two previous broad states. Because we need better accuracy we repeated this experiment in the energy region of interest.

From this experiment we verify the existence of two broad states and because of high resolution in our data it is possible to calculate the ratio  $\frac{\Gamma_n}{\Gamma_{n_0}}$  (where  $\Gamma_n$  is the total neutron partial width and  $\Gamma_{n_0}$  the neutron partial width for the channel with  $^{11}B$  in its ground state). If  $S_n$  is the S - factor for a

$E_R$ (keV)	$E_x$ (keV)	$\Gamma_t$ (keV)	$S_R$ (MeV.b)
391	10391	$\leq 56$	3100*
525	10525	74	11940
574	10574	$\leq 33$	2100*
638	10638	210	4700
910	10910	$\leq 33$	1300*

Table 1: Deduced parameters from the fitting of the  ${}^8\text{Li}(\alpha, n) {}^{11}\text{B}$  reaction experimental data[(\* *Effective S-factor*)]

resonance of  ${}^8\text{Li}(\alpha, n) {}^{11}\text{B}$  for neutron decay in all excited states in  ${}^{11}\text{B}$  and  $S_{n0}$  the S - factor of  ${}^8\text{Li}(\alpha, n0) {}^{11}\text{B}$  for neutron decay to the ground state in  ${}^{11}\text{B}$  we have

$$S_n = S_{n0} \frac{\Gamma_n}{\Gamma_{n0}} \quad (1)$$

that is the upper limit of the S-factor for the  ${}^8\text{Li}(\alpha, n) {}^{11}\text{B}$  reaction.

## 2. Experimental method

The total cross section  $n + {}^{11}\text{B}$  has been measured in a transmission experiment. If  $I_0$  is the counting rate at the detector (fig 1) with no sample, then after insertion of a sample the counting rate is  $I_1 \exp(-\sigma_t d)$  where  $d$  is the density area of the sample. The ratio  $T = \frac{I_1}{I_0}$  is defined as the transmission of the sample, and the total cross section  $\sigma_t$  can be expressed as  $\sigma_t = \frac{1}{d} \ln(T^{-1})$ .

The neutrons production has been done via the  $D(d, n) {}^3\text{He}$  reaction [1,5]. The neutron energy was from 7.3 to 8.5 MeV (with energy steps of 25 keV) and its energy spread was 40 keV. As neutrons detectors are used surface barrier silicon detectors [5]. In our experimental setup (fig. 2) we had placed one more Si-detector in front of the target. For each neutron energy we had two measurements. One with target boron between two detectors and one more with out target. In measurement with out target, the ratio  $R$  of the two detectors' counts is a quantity that depends on the neutron energy, the geometry and is independent of neutrons flux. The product of the ratio  $R$  with the front detector's counts - in the measurement with the target between the two detectors - gives the counts of the back detector if the target did not exist, corrected for possible neutron flux fluctuations. The front detector had 50  $\mu\text{m}$  thickness and  $150 \text{ mm}^2$  area, while the back 150  $\mu\text{m}$  thickness and  $100 \text{ mm}^2$

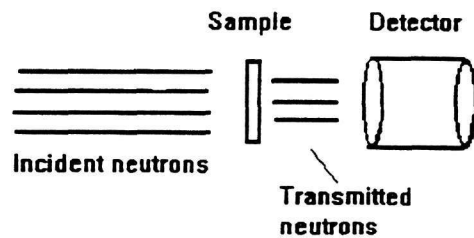


Figure 1: Principle of a transmission experiment

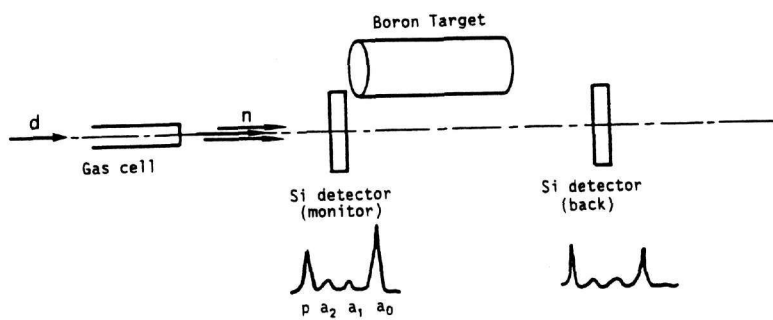


Figure 2: The experimental setup

$E_n^{lab}$ (keV)	$E_x$ (keV)	$\Gamma_t$ (keV)	$\sigma_R$ (b)
7361	10116	$\leq 38$	0.13
7431	10181	41	0.24
7566	10304	56	0.25
7652	10383	$\leq 38$	0.06
7806	10525	78	0.21
7848	10563	$\leq 38$	0.19
7930	10640	200	0.30
8252	10939	$\leq 38$	0.10
8342	11017	$\leq 38$	0.15
8390	11060	$\leq 38$	0.17

Table 2: Parameters from the fitting of the  $n + {}^{11}B$  total cross section experimental data

area. The target was 25 gr natural boron(20%  ${}^{10}B$ , 80%  ${}^{11}B$ ), and with XRF analysis it was calculated 97.5% in boron and 2.5% in iron oxide and other heavy metal oxide. In the  $\sigma_t$  calculation, the  ${}^{10}B$  content of target has been considered, using the total neutron cross section in  ${}^{10}B$  which in this energy region is constant (1.5 b) [3,4]. Also there has been correction for in scattered neutrons but this effect was small (3 or 4%).

### 3. Analysis and Results

In fig. 3, it shown all total cross sections measurements. These data were fitted with several Breit-Wigner formulas,

$$\sigma(E) = \sigma(E_R) \frac{P_1^l(E)}{P_1^l(E_R)} \frac{P_2^l(E)}{P_2^l(E_R)} \frac{\Gamma_t^2}{4(E - E_R)^2 + \Gamma_t^2} \quad (2)$$

plus a linear background. Because of the high neutron energies the neutron penetrability ratios are almost equal to unit, therefore the accepted approximation  $l_n = 2$ , reflects the contribution of this term, even though the value of  $l_n$  is different. The results of the fit consist of ten resonances in the region of interest, and the values of its parameters ( $\sigma_R$ ,  $E_R$ ,  $\Gamma_t$ ) are found in table 2.

Since S-factor for the  ${}^8Li(\alpha, n_0){}^{11}B$  at resonance is given by

$$S_R = 0.197 \cdot (2J + 1) \cdot \exp\left[\frac{306.9}{\sqrt{E_R}}\right] \frac{\Gamma_\alpha(E_R) \cdot \Gamma_{n_0}(E_R)}{\Gamma_t^2(E_R)} \quad (3)$$

	${}^9\text{Be}({}^7\text{Li},\alpha)$ ${}^{10}\text{B}(t,p)$ <sup>(6)</sup>	${}^9\text{Be}(\alpha,p)$ <sup>(7)</sup>	$n + {}^{11}\text{B}^{(3)}$	${}^8\text{Li}(\alpha,n_o)$	Present work
$E_x$	10435	10420	—	10391	10383
$\Gamma_t$	75	115	—	$\leq 56$	$\leq 38$
$E_x$	—	—	10530	10525	10525
$\Gamma_t$	—	—	65	74	78
$E_x$	10580	10572	—	10574	10563
$\Gamma_t$	$\leq 30$	10	—	$\leq 33$	$\leq 38$
$E_x$	—	—	10620	10638	10640
$\Gamma_t$	—	—	$\geq 200$	210	200
$E_x$	10887	10900	—	10910	10939
$\Gamma_t$	30	30	—	$\leq 33$	$\leq 38$

Table 3: Levels of the  ${}^{12}\text{B}$  observed in  ${}^8\text{Li}(\alpha,n_o)$  and  $n + {}^{11}\text{B}$  total cross section experiments, in comparison with other references ( $E_x, \Gamma_t$  in keV)

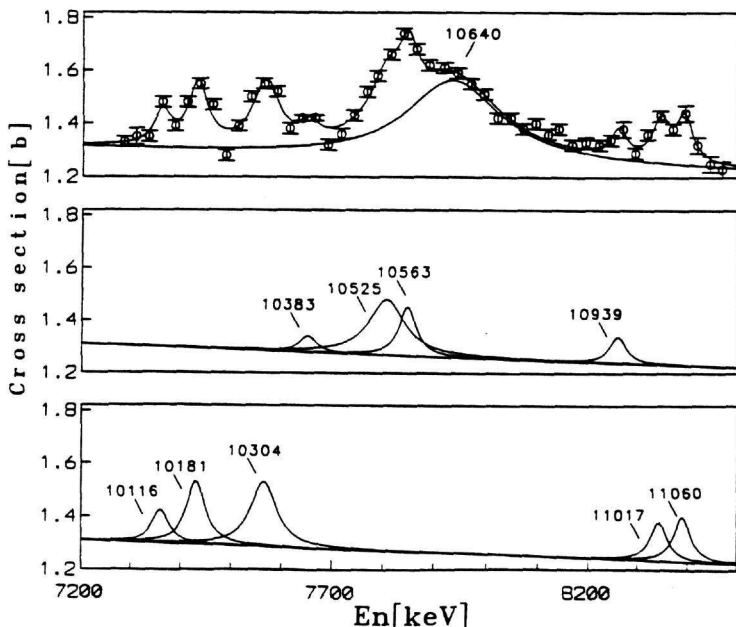


Figure 3: The total neutron cross section of  ${}^{11}\text{B}$ . The solid lines represent the fitting curve and the resonance shapes

$E_R$ (keV)	$\Gamma_{n+no}/\Gamma_{n0}$
391	$\leq 3.0$
525	1.6
574	1.3
638	1.2
910	$\leq 2.0$

Table 4: The ratio  $\Gamma_{no+n}/\Gamma_{no}$  for each resonance

$E_R$ (keV)	$N_A <\sigma v> (\text{cm}^3 \text{mol}^{-1} \text{s}^{-1})$	$\Gamma_{n+no}/\Gamma_{n0}$
391	$1.10 \cdot 10^6 T_9^{-1.5} \exp\left[\frac{-4.33}{T_9}\right]$	$\leq 3.0$
525	$2.10 \cdot 10^7 T_9^{-0.8} \exp\left[\frac{-5.42}{T_9}\right]$	1.6
574	$6.79 \cdot 10^6 T_9^{-1.5} \exp\left[\frac{-6.66}{T_9}\right]$	1.3
638	$1.38 \cdot 10^7 T_9^{0.31} \exp\left[\frac{-5.12}{T_9}\right]$	1.2
910	$5.87 \cdot 10^7 T_9^{-1.5} \exp\left[\frac{-10.56}{T_9}\right]$	$\leq 2.0$

Table 5: Reaction rate for each resonance

and the cross section for the  $^{11}\text{B}(\text{n},\text{n})^{11}\text{B}$  for a resonance from

$$\sigma_R = \frac{358.1}{E_n} \cdot (2J + 1) \cdot \frac{\Gamma_{no+n}(E_R) \cdot \Gamma_{no}(E_R)}{\Gamma_t^2(E_R)} \quad (4)$$

using the relations for total and partial widths

$$\Gamma_t = \Gamma_\alpha + \Gamma_{no} + \Gamma_n$$

$$\Gamma_i^l = 2\gamma_i^2 P_l^i \theta_i^2 \text{ with } \gamma_i^2 = \frac{3}{2} \frac{h^2}{\mu R^2}$$

we can calculate easily the ratios  $\Gamma_n/\Gamma_{no}$  for every resonance.

*3.1 Reaction rates :* In case of a broad resonance the reaction rate of the  $^8\text{Li}(\alpha,\text{n})^{11}\text{B}$  reaction is given by the numerical integration of the following relation [8]

$$N_A <\sigma v> = N_A \left( \frac{2\pi}{\mu kT} \right)^{3/2} \int_0^\infty S(E) \cdot \exp\left[-\frac{E}{kT} - \frac{b}{E^{1/2}}\right] dE \quad (5)$$

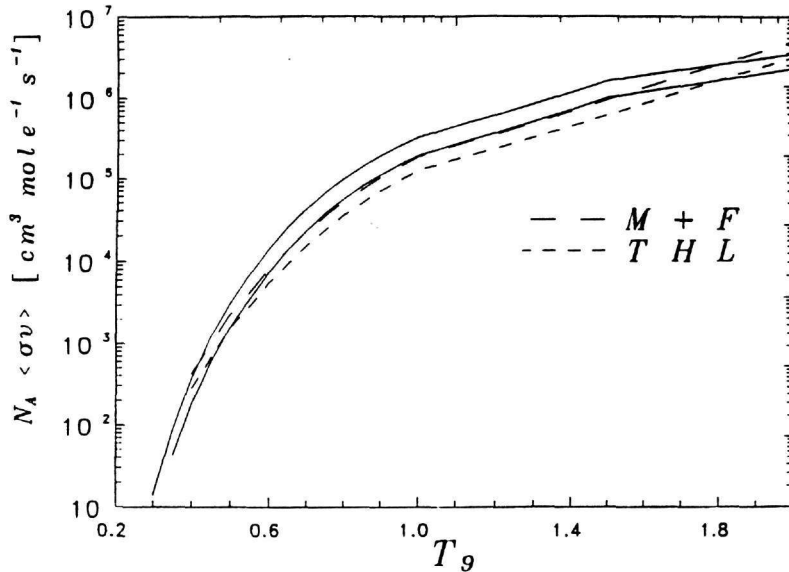


Figure 4: The upper and lower limit of stellar reaction rate for the  ${}^8\text{Li}(\alpha, \text{n}){}^{11}\text{B}$  reaction (solid lines) from this work together with the theoretical values (dashed lines)

for various values of  $T_9$ . The results of the numerical integration have been fitted with the analytic form

$$N_A < \sigma v > = A_1 T_9^m \exp\left[-\frac{A_2}{T_9}\right]$$

and thus we have the reaction rate of these broad resonances as a function of temperature. In case of a narrow resonance we have [8] the analytic form :

$$N_A < \sigma v > = N_A \left(\frac{2\pi}{\mu k T}\right)^{3/2} h^2 (\omega \gamma)_R \exp\left[-\frac{E_R}{k T}\right] \quad (6)$$

or

$$N_A < \sigma v > = A_1 T_9^{-1.5} \exp\left[-\frac{A_2}{T_9}\right]$$

In table 5 we list the stellar reaction rate of each resonance as a function of  $T_9$  and multiplying with  $\Gamma_{no+n}/\Gamma_{no}$  ratio we take an estimation of total reaction rate.

In fig.4 is shown the total reaction rate at  $T_9 = (.2, 2)$  in comparison with theoretical estimates of Malaney and Fowler [9], and Thielmann et al [10]. At  $T_9 = 1$  the avarage value  $2.5 \pm .5 \ 10^5 \text{ cm}^3 \text{ s}^{-1} \text{ mole}^{-1}$  is larger than the theoretical estimates ( $1.9 \ 10^5$  [9],  $1.2 \ 10^5$  [8]), that underestimated the rate of this crucial reaction in primordial nucleosynthesis calculations.

### References

- [1] T. Paradellis, S. Kossionides, G. Doukellis, X. Aslanoglou, P. Assimakopoulos, A. Pakou, C. Rolfs and K. Langange, *Z. Phys.* **A337**, 211, (1990).
- [2] T. Paradellis, G. Doukellis, G. Galios, S. Kossionides, X. Aslanoglou, P. Descouvemont, S. Schmidt and C. Rolfs, *Proceedings of the 2<sup>nd</sup> International Symposium on Nuclear Astrophysics. Edited by F. Kappeler and K. Wissak, Inst. of Physics Publication Conference Series*, p.181 (1993).
- [3] D. B. Fossan, R. L. Walter, W. E. Wilson and H. H. Barschall, *Phys. Rev.* **123**, 209, (1961).
- [4] G. F. Auchampaugh, S. Plattard and N. W. Hill *Nucl. Sc. and Engin.* **69**, 30, (1979)
- [5] G. Doukellis, T. Paradellis and S. Kossionides *Nucl. Instr. and Meth.* **A327**, 480, (1993).
- [6] F. Ajzenberg - Selove *Nucl. Phys.* **A 433**, 1, (1985)
- [7] R. N. Boyd, I. Tanihata, N. Inabe, T. Kubo, T. Nakagawa, T. Susuki, M. Yonokura, X. X. Bai, K. Kimura, S. Kubono, S. Shimoura, H. S. Xu and D. Hirata *Phys. Rev. Lett.* **68**, 1283, (1992).
- [8] C. Rolfs and W. S. Rodney, *Cauldrons in the Cosmos* (University of Chicago Press, Chicago, 1988).
- [9] R. Malaney and R. W. Fowler *Ap. J. Lett.* **345**, 15, (1989).
- [10] F. K. Thielmann, M. Arnould and J. W. Truran *Advances in Nuclear Astrophysics (Gif sur Yvette: Frontiers)* p.525, (1987).